Eur. Phys. J. B **15**, 331–334 (2000)

THE EUROPEAN PHYSICAL JOURNAL B

EDP Sciences

Surface tension effects in the zero gravity inflow of a drop into a fluid

S. Residori[a], E. Pampaloni[b], P.K. Buah-Bassuah[c], and F.T. Arecchi[d]

Istituto Nazionale di Ottica, Largo E. Fermi 6, 50125 Firenze, Italy

Received 31 August 1999

Abstract. As a drop of fluid is deposited on the surface of a miscible fluid (that we call the solvent), it undergoes a strong pulling due to its surface rupture and it acquires a kinetic energy independently of gravity. For the drop and the solvent being of the same fluid we observe a drop injection at an initial velocity which scales as the square root of the surface tension of the drop against air. Once injected, the drop develops a transverse instability giving rise to an expanding ring. Viscosity terminates the process and stops the ring. We show that the final ring height follows a scaling law whereas two asymptotical scaling regimes can be identified for the ring radius.

PACS. 47.20.-k Hydrodynamic stability – 68.10.-m Fluid surfaces and fluid-fluid interfaces

A century after the first report by Thomson [1], the problem of a drop falling in a lighter miscible fluid has been recently reconsidered [2], showing that the process of the drop break-up is essentially ruled by two nondimensional numbers: the fragmentation number, $F = g\Delta\rho V/\mu D$, and the Schmidt number, $Sc = \nu/D$, where g is the gravity acceleration, $\Delta\rho$ the density difference between the drop and the solvent, V the drop volume, $\nu = \mu/\rho$ the kinematic viscosity, ρ the solvent density and D the diffusion constant of the drop into the solvent.

Notice that F and Sc are, respectively, the analogous of the Rayleigh and Prandtl number in convective instabilities, with inertia coming from the density difference and dissipation due to viscosity and diffusion of the concentration gradient. Even if this description in terms of balance between inertia and dissipation has caught some of the essential features of the phenomenon, such as its multifractal nature [3], many questions still remain unanswered.

For example, the fact that the process of break-up is not, in general, observed for immiscible fluids still has no clear explanation. Actually, a break-up into two fragments has been recently observed in one experiment with two immiscible fluids [4], but this observation requires the drop being loaded with some surfactant and travelling such a long distance as 2 m. It is clear that surface tension plays some important role which has never been addressed before and, even in the case of miscible fluids, it is reasonable to ask whether or not we should consider some sort of transient surface tension [5].

Moreover, the hydrodynamics of the process is not yet resolved. The complexity of the problem arises from the simultaneous presence of two hydrodynamic instabilities, Kelvin-Helmoltz (KH) and Rayleigh-Taylor (RT), due, respectively, to the presence of a velocity gradient and of a density difference. We infer from the experimental observations that the KH instability is predominant in the earlier stages of the process, when the drop, injected into the solvent, develops a vortex which expands horizontally into a ring. Once the ring developed, RT starts to act at the interface between the ring and the solvent, where an undulation begins to be amplified until a break-up into secondary droplets takes place. The process can replicate itself if the velocity gradient and the density difference are still large enough for the fragmentation number to be greater than its critical value [2]. Eventually, the process stops as viscous dissipation and concentration diffusion overcome the KH and RT mechanisms.

In this paper, we report experiments done at zero density difference, that is, for the drop and the solvent being of the same fluid. The interest of our observations is twofold. First, getting away of RT we are able to investigate unambiguously the early stage of the process, that is, the ring formation. Then, we show for the first time that the process of drop injection is strongly related to the initial surface tension of the drop against air and that the drop falls into the solvent not because of gravity but because of a strong energy release coming from the rupture of an interface.

The experimental setup consists of a glass cell with a base of $7 \times 7\,\mathrm{cm}^2$ and 20 cm high, mounted on a rigid metallic support. On the top of the cell we mount a

[a] I.N.L.N, U.M.R., C.N.R.S, Universit de Nice-Sophia Antipolis, 1361 Route des Lucioles, 06500 Valbonne, France
[b] e-mail: pampa@ino.it
[c] Phys. Dept., University of Cape Coast, Ghana
[d] Also Phys. Dept., University of Florence, Italy

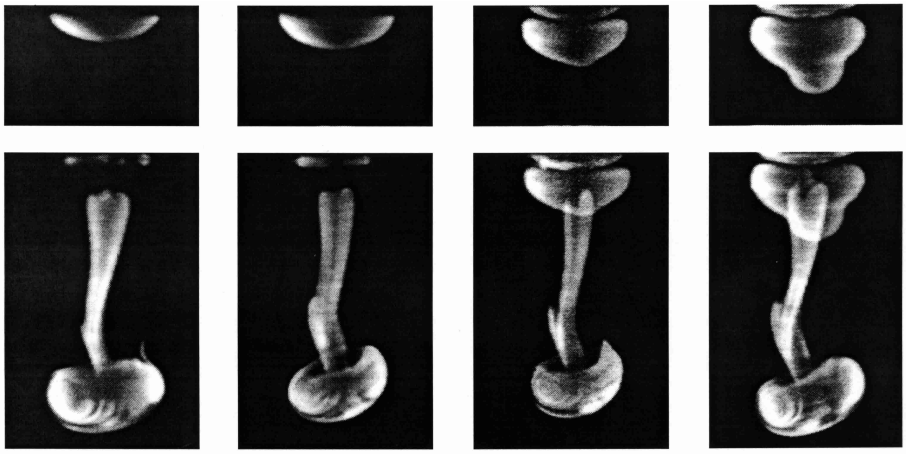

Fig. 1. Side views of the process of drop injection (water into water). The drop volume is 1 μl. The four pairs of images correspond to different events. Each pair represents two successive frames, the lower is 20 ms after the upper one. Comparing the drop size with the distance travelled by the drop we get an initial velocity of roughly 10 cm/s. Notice that two successive frames are superposed in the last two images.

calibrated microsyringe to release the drops. Drop volumes from 0.1 to 50 μl are obtained by using Hamilton microsyringes covering different volume ranges, so that the volume uncertainty is always of the order of a few percents. For each volume range, the syringe needle has an edge with a circular section, the diameter of which is sufficiently large to sustain a pending drop [6]. Notice that in this condition the weight of the drop is balanced by the adhesion of the fluid to the needle walls, so that we can consider that gravity is not playing any role in the whole process. Once the drop is formed at the edge of the needle, by means of a micrometric translation stage, we deposit it with adiabatically zero velocity on the free surface of the solvent. The drop is doped with a small amount of sodium fluorescein dye (10^{-8} mol/l) and is visualized by illuminating the cell with a collimated and expanded argon laser beam. Two CCD cameras are used to register the drop, one camera recording the sideview and the other one recording, from the bottom of the cell, the transverse section. The amount of fluorescein dye is sufficiently low in order not to alter the fluid properties and the dimensions of the cell are large enough in order not to influence the drop dynamics [7].

In Figure 1 we show a few lateral images of a water drop entering water. The process of injection is very fast and the CCD repetition rate (40 ms) does not permit to follow it. In order to catch the essential features of the process, we set the integration time of the CCD to the minimum available for our system, that is 50 μs, and we record images for different events of drop injection, the initial time of each record being different and hazardous at each shot. Then, we extract from the collection of images four successive stages that we show in Figure 1. Looking at the images, we can see that the injection gives rise to a rapid jet incoming from the "point" of contact between the drop and the solvent. The drop fluid enters the solvent through the jet and rolls up into a vortex ring. Our pictures resemble those relative to a falling drop and already reported by ourselves (see [2]) and by other authors [8]. However, this is the first evidence of such a phenomenon for a drop deposited on the fluid surface with zero velocity.

It is this almost instantaneous process of injection that transfers to the drop its initial velocity. Actually, the two fluids being miscible, we can consider that, as soon as the drop touches the solvent surface, a rupture of the drop interface takes place and the energy associated with the interface rupture is converted into kinetic energy. A transverse instability starts to develop almost instantaneously. Indeed, the fluid jet, because of viscous friction, enrolls onto itself giving rise to a vortex ring. The rotational motion of the fluid induces a transverse component of velocity and the ring expands horizontally while travelling downwards. When the kinetic energy is completely dissipated by viscous processes, the ring stops and starts to fade away because of diffusion.

We can use a simple dimensional argument to predict the height h at which the ring stops. By the energy balance $\sigma r^2 = \frac{1}{6}\rho r^3 v_0^2$, between the surface energy $4\pi\sigma r^2$ and the kinetic energy $\frac{4}{3}\pi r^3 \rho \frac{v_0^2}{2}$, where σ is the surface tension of the drop against air and r is the initial drop radius, we find the velocity v_0 that is transferred to the drop fluid at the instant of injection. Once acquired, the initial velocity $v_0 = \sqrt{6\sigma/\rho r}$ is dissipated by viscous processes. We account for dissipation through the Stokes law, so that $\dot{v} = -\gamma\nu v/r^2$, where γ is a shape factor ($\gamma = 6\pi$ for a rigid sphere) [9]. Integrating the Stokes law yields $v(t) = v_0 \mathrm{e}^{-\gamma\frac{\nu}{r^2}t}$ and the maximum height h reached by the drop is $h = \int_0^\infty v(t)\mathrm{d}t = \frac{v_0 r^2}{\gamma\nu} = \frac{v_0}{\gamma}\tau_\nu$, where $\tau_\nu = r^2/\nu$ is the viscous time scale.

Substituting the expression for v_0 and considering that $r \propto V^{\frac{1}{3}}$, where V is the initial drop volume, h can be rewritten as

$$h = \frac{1}{\gamma}\sqrt{\frac{\sigma}{\rho\nu^2}} V^{\frac{1}{2}} \propto l_\nu^{-\frac{1}{2}} r^{\frac{3}{2}} \qquad (1)$$

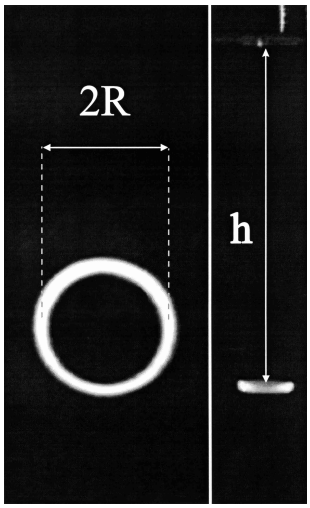

Fig. 2. Lateral and transverse image of the ring stop.

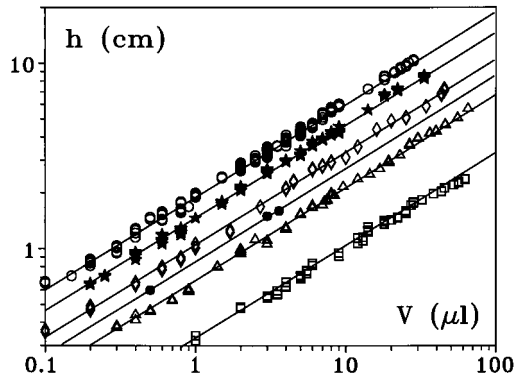

Fig. 3. h as a function of the initial drop volume V for different fluid compositions; empty circles: pure water, stars: 10% glycerin in water (Gly), diamonds: 20% Gly, triangles: 35% Gly, squares: 52% Gly, filled circles: pure ethanol.

where we have included in γ all the geometric form factors and called $l_\nu \equiv \rho\nu^2/\sigma$ a viscous length scale. From now on, we convene to skip numerical factor, since we are interested in scaling relations.

In fact, for a non uniform velocity we should account also for the Basset term [10]. However, the ratio of that term to the Stokes term scales as $r/\sqrt{\nu t}$ and therefore it is negligible for times longer than τ_ν, in our case around 1s. As we go to long times to evaluate the maximum height h, the Basset correction does not modify equation (1) in an appreciable way.

In order to test this prediction, we perform several experiments by using mixtures of distilled water and glycerin at different concentrations. For each fluid mixture and initial drop volume, we register on a videorecorder the entire process, from the drop injection until the ring stop and the onset of diffusion. The lateral and transverse images are combined through a video mixer so that we can follow on the same screen the vertical motion of the drop and the ring formation. By analysing the video tapes, we can catch the images corresponding to the ring stop. On these images, we measure the vertical height h reached by the ring and its radius R (Fig. 2). R is measured as the mean between the inner and the outer radius of the annulus. After each set of measurements, the optical magnification factors are evaluated by recording an image with a millimetric target immersed into the cell and one attached onto the side of the cell. Correspondingly, h and R are then normalized.

In Figure 3 we report the measured height h as a function of the initial drop volume V for different fluid compositions, that is, $0, 10, 20, 35$ and 52% of glycerin. For each fluid composition, $l_\nu^{-1} = \sigma/\rho\nu^2$ is evaluated by substituting for σ, ρ and ν the values tabulated in the current literature [11]. By choosing a reference temperature of 20 °C, which is the room temperature at which we perform the experiments, l_ν^{-1} results to be equal respectively to 72.4, 43.4, 24.9, 9.2 and 2.2×10^4 cm^{-1} for $0, 10, 20, 35$ and 52% of glycerin. The kinematic viscosity is respectively $\nu = 1.0, 1.3, 1.7, 2.7$ and 5.3×10^{-2} cm^2/s. The best fit lines are obtained by inserting into equation (1) the above values for the fluid parameters and by adjusting the geometric factor $\gamma = 15 \pm 1$.

In order to have a further verification of the validity of our description, we perform an experiment by using ethanol as the fluid for the drop and the solvent. In this case, even though the viscosity is lower than the water viscosity, we expect the ring to stop at a smaller h because the surface tension has also been strongly reduced. Unfortunately, we were able to prepare ethanol drops only for a few volumes because of electrostatic problems on the metallic needles. The ethanol having a polar molecule, the metallic needles produce electrostatic forces and the drop remains partially attached at the needle surface; in order to avoid this problem, we had to use a plastic syringe which did not allow to cover a wide range of volumes. However, for the three measured volumes, the data fit quite well our scheme and are well reproduced by equation (1), once we set $\ell_\nu^{-1} = 12.5 \times 10^4$ cm^{-1}, accordingly to the values tabulated for ethanol.

For the same sets of experiments, we report in Figure 4 the measured height R as a function of the initial drop volume V. Two distinct scaling regions can be observed, depending on the volume and viscosity. For small volumes and large viscosities the exponent of the power law fitting the data is close to 2/3 whereas for larger volumes and smaller viscosities data are fit by a 1/3 exponent. Moreover, in this latter case R seems not to depend on the fluid parameters but only on the initial drop volume. As it can be seen in Figure 4, the 1/3 and 2/3 scalings correspond to two asymptotic behaviors, the separation between them depending on the fluid parameters.

We can qualitatively justify the two asymptotic behaviors on the basis of a dimensional argument. The process of drop injection gives rise to a vortical motion of the fluid. The vortex ring transfers part of the initial vertical velocity v_0 in the horizontal direction giving rise to a

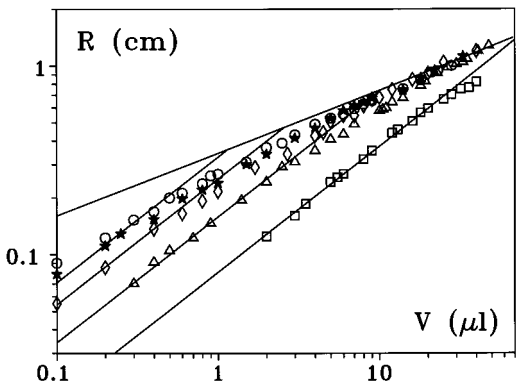

Fig. 4. R as a function of the initial drop volume V for different fluid compositions; empty circles: pure water, stars: 10% Gly, diamonds: 20% Gly, triangles: 35% Gly, squares: 52% Gly. Solid lines have two slopes, namely, 2/3 and 1/3. Each separate data set displays a smooth passage from 2/3 to 1/3 slope as V increases.

transverse component of velocity, $v_\perp$. Once acquired, the horizontal velocity is dissipated by viscosity as the vertical velocity and, because of energy conservation, at the same dissipation rate $1/\tau_\nu$. Therefore, the final ring radius should behave as $R \simeq v_\perp \tau_\nu = v_\perp r^2/\nu$.

We sketch in qualitative terms the sequence of events. As the spherical drop is injected into the quiescent fluid with a velocity v_0, its border starts rotating with respect to the center with the initial velocity v_0, as discussed in the first paper of [2]. Indeed, high friction means that there is a total transfer from vertical to vortical velocity. The initial acceleration of the vortical motion is given by $a = v_0^2/r$; therefore the radial velocity of the vortex built over a characteristic time τ_ν is given by $v_\perp \simeq a\tau_\nu = \frac{v_0^2}{r}\tau_\nu$. It then results $v_\perp \simeq \sigma/\rho\nu$ and $R \simeq r^2/l_\nu = V^{2/3}/l_\nu$, which corresponds to the 2/3 scaling observed for small volumes and large viscosities. On the other hand, if the viscosity is small or the volume is large the rate of the vortex rotation is reduced. Indeed, in this case the boundary layer thickness $\delta = r(Re)^{-\frac{1}{2}} = r(\frac{\nu}{v_0 r})^{\frac{1}{2}}$ (see [9], p. 101) shrinks and hence the transfer from initial velocity v_0 to vortical velocity $v_{\rm eff}$ implies a reduction factor δ/r, that is, $v_{\rm eff} = v_0\delta/r$. Hence $v_\perp = \frac{v_{\rm eff}^2}{r}\tau_\delta$ where $\tau_\delta = \delta^2/\nu$ is the viscous time along the length δ. It follows $v_\perp = \nu/r$, so that $R \simeq v_\perp\tau_\nu = r = V^{1/3}$. Thus, the $V^{1/3}$ law describes the region characterized by small viscosity and large volumes (see pure water).

In conclusion, we have shown that the surface tension σ of the drop against air plays a fundamental role in the initial stage of the dynamics of a drop falling in a miscible fluid. For zero density difference between the drop and the solvent, we have demonstrated that the velocity at which the drop enters the fluid is proportional to $\sqrt{\sigma}$ and we have identified a dissipation length $l_\nu = \rho\nu^2/\sigma$ which permits to rescale the data for h and R to universal power law behaviors.

Notice that the mechanism of drop injection that we have described here is a general one. As long as the two fluid are miscible, it is this mechanism that governs the first stages of the falling drop dynamics, independently of the density difference between drop and solvent. Indeed, we performed some preliminary experiments in the case of a negative density difference and we observed the drop "falling" into the solvent because of the injection. Notice that in the case of immiscible fluids and negative density difference, a drop deposited on the solvent surface undergoes a spreading over this surface [12]. Notice also, that, in the case of positive density difference and immiscible fluids, the absence (or the reduction) of the injection could explain the absence of the transverse instability [1] (or the difficulty to observe it [4]).

We are greatly indebted to S. Fauve for stimulating discussions and precious suggestions. We gratefully acknowledge S. Kumar for having brought to our attention some of the references herein and we thank P. Bianchi for technical assistance in building the cell.

References

1. J.J. Thomson, H.F. Newall, Proc. Royal Soc. London **39**, 447 (1885).
2. F.T. Arecchi, P.K. Buah-Bassuah, F. Francini, C. Perez-Garcia, F. Quercioli, Europhys. Lett. **9**, 333 (1989); F.T. Arecchi, P.K. Buah-Bassuah, C. Perez-Garcia, Europhys. Lett. **15**, 429 (1991); A. Garcimartin, H.L. Mancini, C. Perez-Garcia, Europhys. Lett. **19**, 171 (1992).
3. F.T. Arecchi, P.K. Buah-Bassuah, F. Francini, S. Residori, Phys. Rev. E **54**, 424 (1996).
4. N. Baumann, D.D.J. Joseph, P. Mohr, Y. Renardy, Phys. Fluids A **4**, 567 (1992).
5. D.J. Korteweg, Arch. Neerl. Sci. Ex. Nat. II **6**, 1 (1901); for experimental articles see *e.g.* D.D. Joseph, Eur. J. Mech. B/Fluids **9**, 565 (1990); P. Petitjeans, T. Maxworthy, J. Fluid. Mech. **326**, 37 (1996); E. Lajeunesse, J. Martin, N. Rakotomalala, D.Salin, Phys. Rev. Lett. **79**, 5254 (1997).
6. S. Middleman, *Modeling Axisymmetric Flows* (Academic Press, San Diego, California, 1995).
7. G.H. Ristow, Phys. Rev. E **55**, 2808 (1997).
8. G.K. Batchelor, *An Introduction to Fluid Dynamics* (Cambridge Univ. Press, 1967), Fig. 7.2.3.
9. D.J. Tritton, *Physical Fluid Dynamics* (Oxford University Press, New York, 1988) p. 109.
10. L. Landau, E. Lifshitz, *Fluid Mechanics* (Pergamon, New York, 1967), p. 97.
11. R.C. Weast, *Handbook of Chemistry and Physics* (The Chemical Rubber Co., Cleveland, Ohio, 1971).
12. A.D. Dussaud, S. M. Troian, Phys. Fluids **7**, 1588 (1998) and references therein.